MAXIMIZING DETECTION PERFORMANCE WITH WAVEFORM DESIGN FOR SENSING IN HEAVY SEA CLUTTER

Y. Li, S. P. Sira, A. Papandreou-Suppappola, D. Cochran, L. L. Scharf †

SenSIP Center, Dept. of Electrical Engineering, Arizona State University, Tempe, AZ 85287
†Dept. of Electrical and Computer Engineering, Colorado State University, Fort Collins, CO 80523

ABSTRACT

In this paper, we consider a radar system capable of adaptively adjusting its transmitted waveform to mitigate the effect of the environment and improve detection performance. We thus bring the potential of waveform agility to bear on the challenging problem of target detection in heavy sea clutter. Using a two-stage procedure, we first estimate the statistics of the sea clutter in the vicinity of a predicted target. A phase-modulated waveform is then designed and transmitted so as to maximize the generalized likelihood ratio at the predicted target location, thus improving the signal-to-clutter ratio (SCR). Employing the compound-Gaussian (CG) model, we exploit a subspace-based approach to further mitigate sea clutter and deliver improved detection performance. Simulations illustrate the effectiveness of our method.

Index Terms— agile sensing, sea clutter, target detection, waveform design

1. INTRODUCTION

One of the most important and challenging target detection problems lies in the detection of a target in a highly cluttered environment. In the context of radar, such environments are typical in operation at low grazing angles over heavy seas [1, 2]. Accurate detection of targets in high sea clutter is an important issue in such radar applications as secure navigation, military and coastal security operations, and maritime rescue.

Significant strides have been made in understanding the statistical properties of sea clutter returns [3, 4], in the design of waveforms for clutter mitigation [5, 6], and in processing techniques to alleviate problems caused by heavy sea clutter. Recent efforts entail, for example, time-frequency analysis techniques [7], wavelet-based approaches [8] and neural network-based approaches [9].

The flexibility afforded by modern waveform generators allows implementation of active sensing systems that can select, and even design, their transmitted waveforms on-the-fly. Such systems can tailor the waveform to improve detection performance by minimizing the impact of the environment, to improve tracking performance by obtaining target information that optimally contributes to the current target state estimate, and to improve target recognition performance. Efforts to incorporate dynamic waveform design to improve detection performance include [10, 11, 12, 13].

In this work, we further develop and improve upon a dynamic waveform design method [13] that seeks to design the next transmitted waveform to improve detection performance at a predicted target location. Specifically, we express the generalized likelihood ratio test (GLRT) for the putative target-containing range bin as a function of the autocorrelation function of a template waveform and the variance of the sea clutter in its neighborhood. A maximization of the GLRT over the waveform parameters is then carried out to yield a design that minimizes the contribution of sea clutter to the return from the target thus improving the SCR in that range bin and resulting in better detection performance. We use the well-established compound-Gaussian model for sea clutter returns and estimate its time-varying statistics using the Expectation-Maximization (EM) algorithm. We also incorporate subspace-based techniques to exploit the difference in the short time correlation of the sea clutter and the target. Furthermore, we provide simulation results to demonstrate that our approach leads to appreciable improvement in detection performance.

The paper is organized as follows. In Section 2, we briefly describe the system and sea clutter models as well as the estimation of clutter statistics. We also describe the subspace-based clutter suppression method. We propose our dynamic waveform design method in Section 3, and present simulation results in Section 4.

2. SYSTEM AND SEA CLUTTER MODELS

2.1. System Model

Our waveform-agile detection methodology uses a two-stage procedure to develop a design of the transmitted waveform to minimize the influence from heavy sea clutter to improve detection performance. The first stage is used to estimate time-

This work was partly supported under MURI Grant No. AFOSR FA9550-05-1-0443 and by the DARPA Waveforms for Active Sensing Program under NRL grant N00173-06-1-G006.

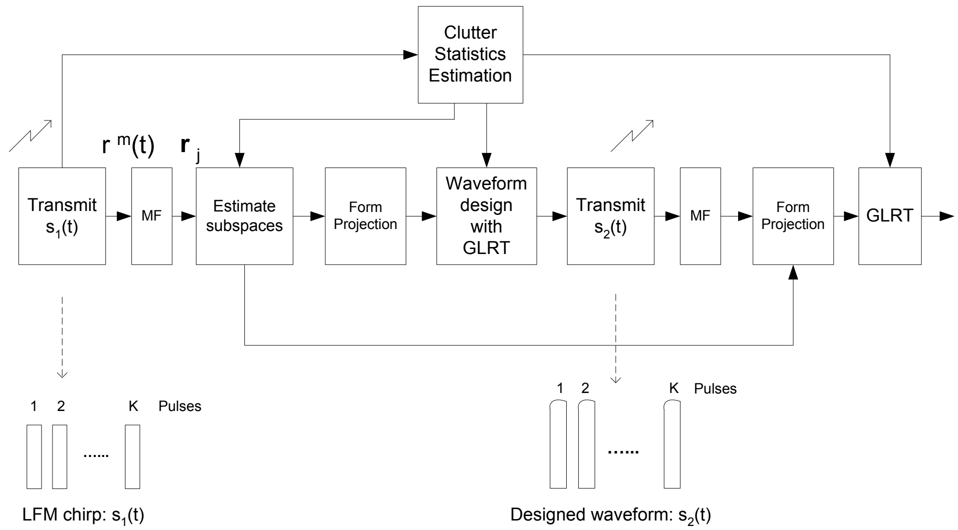

Fig. 1. Block diagram of the proposed waveform-agile detection system.

varying clutter statistics, while in the second stage the designed waveform is transmitted and its returns are processed to yield the final detection. We consider a medium pulse repetition frequency (PRF) radar that periodically *dwells* on a given area of the ocean surface. Each dwell of the radar is assumed to consist of two sub-dwells, during each of which K identical pulses are transmitted. During Sub-dwell 1, a linear frequency-modulated (LFM) chirp $s_1(t)$ is transmitted, while the waveform $s_2(t)$ in Sub-dwell 2, is a dynamically designed phase-modulated waveform. The system block diagram is shown in Fig. 1.

In each sub-dwell, the complex reflectivity of the ith scatterer to the K pulses is denoted as $\mathbf{y}_i = [y_i^0, \cdots, y_i^{K-1}]^T$, where ^{T} denotes transpose. The received signal, $r^m(t)$ in Fig. 1, at the mth pulse, $m = 0, 1, \cdots, K-1$, is given by:

$$\begin{aligned} r^m(t) &= b^m s(t-\tau_0)\exp(j2\pi\nu_0 t) + \\ &\quad \sum_i y_i^m s(t-\tau_i)\exp(j2\pi\nu_i t) + n(t), \quad (1) \end{aligned}$$

where b^m, τ_0 and ν_0 are the complex reflectivity at the mth pulse, delay and Doppler shift, respectively, of the target (if present), τ_i and ν_i are the delay and Doppler shift of the ith scatterer, and $n(t)$ is additive noise. We assume a Swerling I target with complex reflectivity $\mathbf{b} = [b^0, b^1, \cdots, b^{K-1}]$ that follows a complex Gaussian distribution $\mathbf{b} \sim \mathcal{CN}(0, \sigma^2\mathbb{I}_K)$, where $\mathbb{I}_K$ denotes the $K \times K$ identity matrix. Since we only consider transmitted signals of very short duration, the Doppler resolution is very poor. Therefore, we completely ignore Doppler processing and restrict our attention to delay or range estimation alone. Further, we will assume that the clutter is the dominant source of interference and henceforth ignore the effect of the additive noise $n(t)$ in (1).

After sampling and matched-filtering the received signal $r^m(t)$, the vector of matched-filtered outputs at the jth delay or range bin is denoted by $\mathbf{r}_j \in \mathbb{C}^{K\times 1}$ and is given by

$$\mathbf{r}_j = \mathbf{b} z_s[j-n_0] + \sum_{n=-(N_s-1)}^{N_s-1} z_s[n]\mathbf{y}_{j+n}, \qquad (2)$$

where n_0 is the index of the range bin where the target is located, $z_s[n]$, $|n| < N_s$ is the autocorrelation function, and N_s is the length of the transmitted signal.

2.2. Sea Clutter Model

When a radar has adequately high resolution to resolve fine structure on the sea surface, sea clutter returns are not well modeled by a Gaussian distribution [4]. The heavier-tailed compound-Gaussian model [3] has received widespread attention and support, both theoretical and empirical, in radar signal processing to describe the statistics of clutter echoes. In this model, reflections from the sea surface are believed to be due to two components corresponding to distinct phenomena. The small-scale structure, characterized by short correlation time and spatial independence, is referred to as the speckle. Speckle is a rapidly fluctuating component accounting for local scattering, which is complex Gaussian distributed. The large-scale structure, or texture, is a slowly fluctuating component that modulates the speckle. The texture reflects the local mean power of the clutter and depends on sea state, wind, and swell and exhibits both spatial and temporal correlation. It has been variously modeled as having gamma, inverse gamma, Weibull, or log-normal distribution.

According to the compound-Gaussian model, the reflectivity of the ith scatterer is [14] $\mathbf{y}_i = \sqrt{\mathcal{T}_i}\boldsymbol{\mathcal{S}}_i$, where the speckle $\boldsymbol{\mathcal{S}}_i$ is a stationary complex Gaussian process with zero mean and covariance matrix $\mathbf{\Sigma} \in \mathbb{C}^{K\times K}$ and the texture is $\mathcal{T}_i \geq 0$. Therefore, given $\mathcal{T}_i$ and $\mathbf{\Sigma}$, $\mathbf{y}_n \sim \mathcal{CN}(0, \mathcal{T}_n\mathbf{\Sigma})$.

From analysis of experimental sea clutter data collected at the Osborne Head Gunnery Range (OHGR) with the McMaster university IPIX radar [15], it has been found that the speckle is correlated over 1-5 ms while the texture remains correlated over 50-60 s [16, 17, 13]. If the PRF is high enough to ensure that the K pulses in a sub-dwell are transmitted with a duration of 1-2 ms, we can expect that the clutter returns will not be independent so that $\mathbf{\Sigma} \neq \mathbb{I}_K$ and that the texture variables are practically constant across a complete dwell. These assumptions accordingly inform our method for the estimation of the clutter statistics.

2.3. Estimation of Clutter Statistics

We utilize the returns from Sub-dwell 1 to estimate the sea clutter statistics in the vicinity of a predicted target location. Assuming that the target is predicted in range bin j, we seek to estimate

$$\Theta = \{\mathcal{T}_{j-2(N_s-1)}, \cdots, \mathcal{T}_j, \cdots, \mathcal{T}_{j+2(N_s-1)}, \mathbf{\Sigma}\}.$$

From (2), we note that there is a many-to-one mapping between the clutter scatterers and the matched-filtered vector. Therefore, we can only obtain a maximum likelihood estimate

$$\hat{\Theta} = \arg\max_{\Theta} \; p(\mathbf{y}; \Theta), \tag{3}$$

where $\mathbf{y} = [\tilde{\mathbf{y}}^H_{j-2(N_s-1)}, \cdots, \tilde{\mathbf{y}}^H_j, \cdots, \tilde{\mathbf{y}}^H_{j-2(N_s-1)}]^H$ and $\tilde{\mathbf{y}}_j = \mathbf{y} + \mathbf{b}\delta[j-n_0]$, with $\delta[\cdot]$ denoting the Kronecker delta. The estimate in (3) can be found using the EM algorithm [18]. This algorithm iterates

$$\begin{aligned} U(\Theta, \hat{\Theta}^{(l)}) &= E\{\ln p(\mathbf{y}; \Theta) | \mathbf{r}, \hat{\Theta}^{(l)}\} \\ \hat{\Theta}^{(l+1)} &= \arg\max_{\Theta} U(\Theta, \hat{\Theta}^{(l)}) \end{aligned}$$

until such time the variation in the estimate falls below a preset threshold [13].

2.4. Clutter Suppression

We use a subspace-based clutter suppression method to initially improve detection performance as in [19, 20], with the assumption that most of the energy in the clutter returns is concentrated in a low-rank subspace. The orthogonal projection of the received signal on the clutter subspace should therefore present a higher SCR leading to improved detectability. From (2), the covariance matrix of the matched-filtered return $\mathbf{r}_j$ is [13]

$$\mathbf{R}_j = E\{\mathbf{r}_j \mathbf{r}_j^H\} = \sigma^2 \mathbb{I}_k |z_s[j-n_0]|^2 + \mathbf{\Sigma}\beta_j, \tag{4}$$

where

$$\beta_j = \sum_{n=-(N_s-1)}^{N_s-1} \mathcal{T}_{j+n} |z_s[n]|^2, \tag{5}$$

is a scalar that depends on the waveform. Note that the eigenspace of the clutter is thus identical to that of the speckle component. Therefore, an estimate of the clutter subspace is obtained from the estimated speckle covariance matrix $\hat{\mathbf{\Sigma}}$.

Let N_e be the number of the largest eigenvalues of $\hat{\mathbf{\Sigma}}$ that contribute a large percentage P of its total energy (e.g., we choose $P = 99.99\%$ in our simulations). Let Q_c be the $K \times N_e$ matrix, whose columns are the corresponding eigenvectors, and $Q_c^\perp$ be the $K \times K'$ matrix, whose columns are the remaining eigenvectors of $\hat{\mathbf{\Sigma}}$, where $K' = K - N_e$. By forming the projection

$$\mathbf{r}_j^\perp = Q_c^{\perp H} \mathbf{r}_j, \tag{6}$$

we obtain a clutter-suppressed received signal. In the next section, we describe the detector that operates on this signal.

3. WAVEFORM DESIGN WITH GLRT DETECTION

With respect to range bin j, let $\mathcal{H}_0$ denote the hypothesis that only clutter is present, and let $\mathcal{H}_1$ denote the presence of both clutter and target. The GLRT detector decides $\mathcal{H}_1$ if

$$\Lambda_j^{GLRT} = \ln \frac{p(\mathbf{r}_j^\perp | \mathcal{H}_1, \hat{\boldsymbol{\mathcal{T}}}, \hat{\mathbf{\Sigma}}, \hat{\sigma}^2)}{p(\mathbf{r}_j^\perp | \mathcal{H}_0, \hat{\boldsymbol{\mathcal{T}}}, \hat{\mathbf{\Sigma}})} > \gamma, \tag{7}$$

where γ is a threshold that achieves a desired false alarm probability. If $\mathcal{H}_0$ is true, (4) can be reduced to $\mathbf{R}_j = \hat{\beta}_j \hat{\mathbf{\Sigma}}$ since $|z_s[j-n_0]| \ll 1$ and the SCR is low. From (6), the covariance matrix of $\mathbf{r}_j^\perp$ is

$$\mathbf{C}_w = \hat{\beta}_j \hat{Q}_c^{\perp H} \hat{\mathbf{\Sigma}} \hat{Q}_c^\perp.$$

If $\mathcal{H}_1$ is true, the covariance matrix can be expressed as

$$\begin{aligned} \mathbf{C}_{sw} &= \hat{Q}_c^{\perp H} \hat{\sigma}^2 \mathbb{I}_K \hat{Q}_c^\perp + \hat{\beta}_j \hat{Q}_c^{\perp H} \hat{\mathbf{\Sigma}} \hat{Q}_c^\perp \\ &= \hat{\sigma}^2 \mathbb{I}_{K'} + \hat{\beta}_j \hat{Q}_c^{\perp H} \hat{\mathbf{\Sigma}} \hat{Q}_c^\perp. \end{aligned}$$

Since both probability density functions in (7) are complex Gaussian with zero mean, the GLRT in (7) reduces to

$$T(\mathbf{r}_j^\perp) = \mathbf{r}_j^{\perp H} \mathbf{C}_w^{-1} \hat{\sigma}^2 \mathbf{C}_{sw}^{-1} \mathbf{r}_j^\perp \gtrless \gamma. \tag{8}$$

Using the eigen-decomposition $\mathbf{C}_w = V_w \Lambda_w V_w^H$, where V_w is a unitary matrix of the eigenvectors of $\mathbf{C}_w$ and Λ_w is a diagonal matrix of its eigenvalues $\lambda_w^n, n = 0, \cdots, K'-1$, (8) can be simplified as

$$T(\tilde{\mathbf{r}}_j^\perp) = \tilde{\mathbf{r}}_j^{\perp H} \hat{\sigma}^2 \Lambda_w^{-1} (\mathbb{I}_{K'} + \hat{\sigma}^2 \Lambda_w^{-1})^{-1} \tilde{\mathbf{r}}_j^\perp \gtrless \gamma,$$

where $\tilde{\mathbf{r}}_j^\perp = \Lambda_w^{-1/2} V_w^H \mathbf{r}_j^\perp$. Then,

$$T(\tilde{\mathbf{r}}_j^\perp) = \sum_{n=0}^{K'-1} \frac{\hat{\sigma}^2}{\hat{\sigma}^2 \, \hat{\beta}_j + \lambda_w^n \, \hat{\beta}_j^2} \, |(\lambda_w^n)^{-1/2} \, \mathbf{r}_j^\perp[n]|^2, \tag{9}$$

where $\mathbf{r}_j^\perp[n]$ denotes the nth element of $\mathbf{r}_j^\perp$.

3.1. Waveform Design

At the end of Sub-dwell 1, the detector in (9) provides a predicted target location for the waveform design for Sub-dwell 2. Our aim is to design a waveform that maximizes detection performance in Sub-dwell 2. Recall that $\hat{\beta}_j$ depends on the transmitted waveform. We therefore seek to design $s_2(t)$ so that $T(\tilde{\mathbf{r}}_j^{\perp})$ is maximized in Sub-dwell 2. Our approach represents a formal mechanism of designing the waveform in contrast to [13], where it was approached in a relatively ad-hoc manner to minimize the out-of-bin clutter contributions to the return from the predicted target range bin.

The waveform $s_2(t)$ is chosen to be a unimodular phase-modulated waveform

$$s_2(t) = \exp\left(j\boldsymbol{\psi}(t)\right),\ 0 \leq t \leq T_s,$$

where the phase modulation is expanded in terms of an orthogonal set of basis functions $\{\boldsymbol{\psi}_i\}$ as $\boldsymbol{\psi}(t) = \sum_{i=1}^{N_s} \mu_i \psi_i(t)$ and

$$\psi_i(t) = \begin{cases} 1, & (i-1)\Delta T \leq t \leq i\Delta T \\ 0, & \text{otherwise,} \end{cases}$$

where T_s and ΔT is the pulse duration and sampling interval, respectively. Then, the autocorrelation function of the signal is given by

$$z_s[n] = \frac{1}{N_s} \sum_{i=1}^{N_s - n} \left[\cos(\mu_{n+i} - \mu_i) + j\sin(\mu_{n+i} - \mu_i)\right]. \tag{10}$$

We propose to design $s_2(t)$ by determining the solution of

$$\arg\max_{\boldsymbol{\mu}} \Lambda_j^{GLRT}, \tag{11}$$

where $\boldsymbol{\mu} = [\mu_1, \cdots, \mu_{N_s}]$. With $\hat{\beta}_j$ defined similarly to β_j in (5) and using (9) and (10), we can approximately solve (11) in two steps. First we use a gradient descent algorithm to maximize the likelihood ratio with respect to the scalar $\hat{\beta}_j$, which is a function of the waveform, to obtain

$$\beta_j^* = \arg\max_{\hat{\beta}_j} \Lambda_j^{GLRT}, \tag{12}$$

subject to the constraint $\beta_j^* \geq \hat{\mathcal{T}}_j$. The weights $\boldsymbol{\mu}$ are then obtained by a second gradient descent algorithm as

$$\boldsymbol{\mu}^* = \arg\min_{\boldsymbol{\mu}} |\hat{\beta}_j - \beta_j^*|. \tag{13}$$

The necessary derivatives are provided below. From (5) and (10), we have

$$\begin{aligned} \hat{\beta}_j &= \frac{1}{N_s^2} \sum_{n=-(N_s-1)}^{N_s-1} \hat{\mathcal{T}}_{j+n} \Big\{ N_s - n \\ &+ \sum_{l=1, l\neq i}^{N_s-n} \sum_{i=1}^{N_s-n} \cos(\mu_{n+i} - \mu_{n+l} - \mu_i + \mu_l) \Big\}. \end{aligned} \tag{14}$$

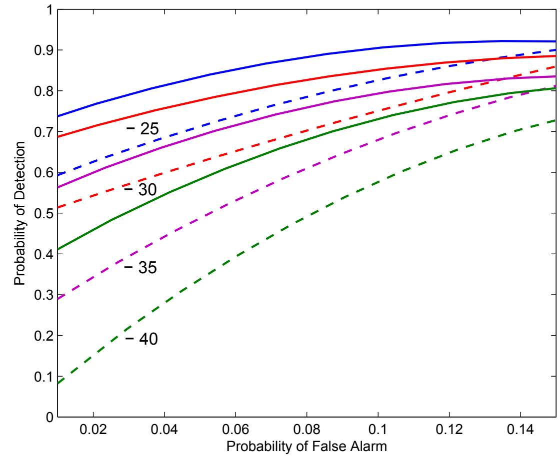

Fig. 2. ROC curves with different SCR values. The numbers indicate SCR values in dB. Dashed lines are ROC curves using a fixed LFM chirp (without waveform design); solid lines are ROC curves using proposed dynamic method (with waveform design).

Differentiating (14) with respect to $\boldsymbol{\mu}$, we obtain:

$$\begin{aligned} \frac{\partial \hat{\beta}_j}{\partial \mu_1} = 2\Big[&\sum_{n=1}^{N_s-1} \Big(\sum_{i=1}^{N_s-n} \cos(\mu_{n+i} - \mu_i) \Big) \sin(\mu_{n+1} - \mu_1) \\ - &\sum_{n=1}^{N_s-1} \Big(\sum_{i=1}^{N_s-n} \sin(\mu_{n+i} - \mu_i) \Big) \cos(\mu_{n+1} - \mu_1) \Big] \end{aligned}$$

and for $p = 2, \cdots, N_s$

$$\begin{aligned} \frac{\partial \hat{\beta}_j}{\partial \mu_p} = 2\Big[&\sum_{n=1}^{N_s-p} \Big(\sum_{i=1}^{N_s-n} \cos(\mu_{n+i} - \mu_i) \Big) \sin(\mu_{n+p} - \mu_p) \\ - &\sum_{n=1}^{p-1} \Big(\sum_{i=1}^{N_s-n} \cos(\mu_{n+i} - \mu_i) \Big) \sin(\mu_p - \mu_{p-n}) \\ - &\sum_{n=1}^{N_s-p} \Big(\sum_{i=1}^{N_s-n} \sin(\mu_{n+i} - \mu_i) \Big) \cos(\mu_{n+p} - \mu_p) \\ + &\sum_{n=1}^{p-1} \Big(\sum_{i=1}^{N_s-n} \sin(\mu_{n+i} - \mu_i) \Big) \cos(\mu_p - \mu_{p-n}) \Big]. \end{aligned}$$

4. SIMULATIONS

In our simulations, we detect a target that moves away from the sensor at approximately 5 m/s in the presence of simulated K-distributed sea clutter. In each simulation consisting of 25 dwells, $K = 10$ pulses of a 1.5 μs duration each are transmitted in each sub-dwell. In Sub-dwell 1, $s_1(t)$ is an LFM chirp with a frequency sweep of 100 MHz. The length of the signal is 150 samples. The pulse repetition interval (PRI) was 100 μs so that the duration of each sub-dwell is 1 ms. An average of 6,000 scatterers were uniformly distributed in range over the extent of each range bin and uniformly in Doppler over [-1, 1] kHz. At a carrier frequency $f_c = 10.4$ GHz, the target Doppler shift is approximately -350 Hz. The clutter amplitudes were sampled from a K-distribution with appropriate correlations [13]. The amplitude of target return was sampled from a zero mean complex Gaussian process with covariance matrix $\sigma^2 \mathbb{I}_K$, where σ^2 was chosen to satisfy the specified SCR values. We define the SCR to be the ratio of the target variance to the *total* clutter power in the range bin.

Figure 2 shows the Monte Carlo averaged receiver operating characteristic (ROC) curves with different SCR values at the end of each sub-dwell. It is thus a comparison of the performance obtained by using the fixed waveform $s_1(t)$ (dashed lines) and the dynamically designed waveform $s_2(t)$ (solid lines). It is apparent that the latter provides more than 5 dB gains in SCR. Note also that the detection performance is reasonable even at very low SCR values. This is due to the exploitation of the orthogonal projection as well as the dynamic waveform design.

5. CONCLUSION

In this paper, we proposed an application to exploit the potential of waveform-agility to improve target detection performance in heavy sea clutter. Using the compound-Gaussian model to describe the clutter statistics we developed a methodology to estimate the clutter power in the neighborhood of a predicted target location. These estimates were first used to estimate the clutter subspace, and an orthogonal projection of the received signal was formed to achieve appreciable clutter suppression. Next, we developed a method to dynamically design a phase-modulated waveform that maximizes the generalized likelihood ratio corresponding to that location or range bin. We applied our method in a simulation study to detect a moving target, and the results demonstrated the benefits of the proposed method over one that uses a non-adaptive, fixed waveform at each transmission.

6. REFERENCES

[1] H. Leung, "Nonlinear clutter cancellation and detection using a memory-based predictor," *IEEE Transactions on Aerospace and Electronic Systems*, vol. 32, pp. 1249–1256, 1996.

[2] P. A. Ffrench, J. R. Zeidler, and W. H. Ku, "Enhanced detectability of small objects in correlated clutter using an improved 2-D adaptive lattice algorithm," *IEEE Transactions on Image Processing*, vol. 6, pp. 383–397, 1997.

[3] K. Ward, C. Baker, and S. Watts, "Maritime surveillance radar Part I: Radar scattering from the ocean surface," *IEE Proceedings F: Communications, Radar and Signal Processing*, vol. 137, pp. 51–62, April 1990.

[4] S. Haykin, R. Bakker, and B. W. Currie, "Uncovering nonlinear dynamics - The case study of sea clutter," *Proceedings of the IEEE*, vol. 90, pp. 860–881, May 2002.

[5] S. M. Sussman, "Least-square synthesis of radar ambiguity functions," *IRE Transactions on Information Theory*, vol. IT-8, Apr. 1962.

[6] D. F. DeLong and E. M. Hofstetter, "On the design of optimum radar waveforms for clutter rejection," *IEEE Transactions on Information Theory*, vol. IT-13, pp. 454–463, Jul. 1967.

[7] T. Thayaparan, "Detection of a manoeuvring air target in sea-clutter using joint time-frequency analysis techniques," *IEE Proceedings–Radar, Sonar and Navigation*, vol. 151, pp. 19–30, Feb. 2004.

[8] G. Davidson and H. D. Griffiths, "Wavelet detection scheme for small targets in sea clutter," *Electronics Letters*, vol. 38, pp. 1128–1130, Sep. 2002.

[9] T. Bhattacharya and S. Haykin, "Neural network-based radar detection for an ocean environment," *IEEE Transactions on Aerospace and Electronic Systems*, vol. 33, pp. 408–420, Apr. 1997.

[10] S. U. Pillai, D. C. Youla, H. S. Oh, and J. R. Guerci, "Optimum transmit-receiver design in the presence of signal-dependent interference and channel noise," *IEEE Transations on Information Theory*, vol. 46, pp. 577–584, Mar. 2000.

[11] B. Friedlander, "A subspace framework for adaptive radar waveform design," in *Proc. Asilomar Conference on Signals, Systems and Computers*, pp. 1135–1195, Oct. 2005.

[12] L. Scharf and A. Pezeshki, "Virtual array processing for active sensing," in *Proc. Asilomar Conference on Signals, Systems, and Computers*, pp. 740–744, Oct. 2006.

[13] S. P. Sira, D. Cochran, A. Papandreou-Suppappola, D. Morrell, W. Moran, S. Howard, and R. Calderbank, "Adaptive waveform design for improved detection of low-RCS targets in heavy sea clutter," *IEEE Journal on Special Topics in Signal Processing*, vol. 1, pp. 56–66, June 2007.

[14] K. J. Sangston and K. R. Gerlach, "Coherent detection of radar targets in a non-Gaussian background," *IEEE Transactions on Aerospace and Electronic Systems*, vol. 30, pp. 330–340, Apr. 1994.

[15] A. Drosopoulos, "Description of the OHGR database," tech. rep., Defense Research Establishment, Ottawa, Dec. 1994.

[16] A. Farina, F. Gini, M. V. Greco, and L. Verrazzani, "High resolution sea clutter data: statistical analysis of recorded live data," *IEE Proceedings on Radar, Sonar and Navigation*, vol. 144, pp. 121–130, Jun. 1997.

[17] W. Stehwien, "Statistics and correlation properties of high resolution X-band sea clutter," in *IEEE International Radar Conference*, pp. 46–51, Mar. 1994.

[18] A. Dempster, N. Laird, and D. Rubin, "Maximum likelihood estimation from incomplete data via the EM algorithm," *Journal of the Royal Statistical Society, Series B*, pp. 1–38, 1977.

[19] J. R. Guerci, *Space-Time Adaptive Processing for Radar*. Norwood, MA: Artech House, 2003.

[20] S. Suvorova, B. Moran, and M. Viola, "Adaptive modeling of sea clutter and detection of small targets in heavy sea clutter," in *IEEE International Radar Conference*, pp. 614–618, 2003.